Received: 27 October 2021 | Revised: 15 December 2021 | Accepted: 16 December 2021

DOI: 10.1002/rcm.9246

RESEARCH ARTICLE

Rapid Communications in Mass Spectrometry WILEY

Differentiation of leucine and isoleucine residues in peptides using charge transfer dissociation mass spectrometry (CTD-MS)

Halle M. Edwards[1] | Hoi-Ting Wu[2] | Ryan R. Julian[2] | Glen P. Jackson[1,3]

[1]C. Eugene Bennett Department of Chemistry, West Virginia University, Morgantown, WV, USA

[2]Department of Chemistry, University of California, Riverside, CA, USA

[3]Department of Forensic and Investigative Science, West Virginia University, Morgantown, WV, USA

Correspondence
G. P. Jackson, C. Eugene Bennett Department of Chemistry, West Virginia University, Morgantown, WV, USA.
Email: glen.jackson@mail.wvu.edu

Funding information
National Institutes of Health, Grant/Award Number: R01-GM114494-01; National Science Foundation, Grant/Award Number: CHE-1710376

Rationale: The function of a protein or the binding affinity of an antibody can be substantially altered by the replacement of leucine (Leu) with isoleucine (Ile), and vice versa, so the ability to identify the correct isomer using mass spectrometry can help resolve important biological questions. Tandem mass spectrometry approaches for Leu/Ile (Xle) discrimination have been developed, but they all have certain limitations.

Methods: Four model peptides and two wild-type peptide sequences containing either Leu or Ile residues were subjected to charge transfer dissociation (CTD) mass spectrometry on a modified three-dimensional ion trap. The peptides were analyzed in both the 1+ and 2+ charge states, and the results were compared to conventional collision-induced dissociation spectra of the same peptides obtained using the same instrument.

Results: CTD resulted in 100% sequence coverage for each of the studied peptides and provided a variety of side-chain cleavages, including *d*, *w* and *v* ions. Using CTD, reliable *d* and *w* ions of Xle residues were observed more than 80% of the time. When present, *d* ions are typically greater than 10% of the abundance of the corresponding *a* ions from which they derive, and *w* ions are typically more abundant than the *z* ions from which they derive.

Conclusions: CTD has the benefit of being applicable to both 1+ and 2+ precursor ions, and the overall performance is comparable to that of other high-energy activation techniques like hot electron capture dissociation and UV photodissociation. CTD does not require chemical modifications of the precursor peptides, nor does it require additional levels of isolation and fragmentation.

1 | INTRODUCTION

Over the past several decades, mass spectrometry has become the preferred method for identifying peptides and proteins in biomedical applications. However, differentiation of isomeric residues in peptides still represents a considerable challenge in tandem mass spectrometry. Collision-induced dissociation (CID), which is the most common method for interrogating peptides, tends to fragment the weakest bonds of a molecule and predominantly results in *b* and *y* ions for peptides. Whereas *b* and *y* ions provide adequate mass information to identify most amino acids in peptides, the formation of *b* and *y* ions is not sufficient to differentiate leucine (Leu) and isoleucine (Ile), which are constitutional isomers. Differentiation of Leu/Ile (Xle) residues is particularly important to the development of monoclonal antibodies as therapeutic drugs to treat autoimmune diseases, cancers and, most recently, COVID-19, because incomplete or inaccurate sequencing can diminish the effectiveness of certain drugs.[1–4]

Many techniques have emerged to provide solutions to adequately and reliably differentiate Xle residues. The formation of metal complexes can provide distinction in dipeptides,[5,6] and special enzymatic reactions can aid in the differentiation of Xle residues in larger peptides.[7] Low-mass (*m*/*z* 86) immonium ions of Xle also can differentiate the two amino acids, but only when there is a single Xle residue present in the peptide precursor.[8] Derivatization and dimethyl labeling can provide some clarity about Xle residues in CID experiments, but this approach requires fragmentation at the MS^3 level.[9] Experiments using consecutive reactions have had success in differentiating Xle residues, but they require adequately abundant peaks of interest for repetitive sequential fragmentation, and they are generally not amenable to the timescales required for on-line analyses with liquid chromatography.[10]

Other fragmentation techniques, like electron capture dissociation (ECD) and electron transfer dissociation (ETD), have emerged as complementary techniques to CID. ECD and ETD both generate abundant *c*/*z* ions, which contrasts with the dominant *b*/*y* ions in CID. However, backbone cleavages alone cannot provide the information necessary to distinguish Leu from Ile. Instead, cleavage of the amino acid side chains can provide the most valuable information for differentiating Xle residues. This secondary fragmentation is observed in several radical-driven fragmentation techniques, such as those that first generate $a^\bullet$ and $z^\bullet$ fragment ions and subsequently fragment into *d* and *w* ions, respectively.[11–14] Recent investigations confirm that the formation of $a^\bullet$ ions proceeds through a nitrogen-centered radical, and *d* ions then form via additional radical migration.[15,16]

For peptides with charge states 2+ or greater, ECD and ETD tend to produce a series of $z^\bullet$ fragment ions, which can be exploited to produce *w* ions through multistage and hybrid techniques like IR-ECD,[17] ETD-CAD,[18,19] ECuvPD,[20] EChcD[20] and EtHCD.[21,22] However, the multistage techniques, except for EtHCD, can be cumbersome because they require manual isolation and fragmentation of each $z^\bullet$ ion of interest. EtHCD is different because it applies supplementary activation to all product ions produced during an ETD event, so it is easier to implement in an automated manner.[21,23] Matrix-assisted laser desorption ionization (MALDI) with in-source decay (ISD) can also generate *d* and *w* ions to help differentiate Xle residues, but MALDI-ISD has fairly limited sequence coverage.[15,24,25]

Hot electron capture dissociation (HECD), which operates with electrons of higher kinetic energy than traditional ECD, can produce abundant *w* ions at the MS^2 level,[26–29] as demonstrated by the neutral losses of $^\bullet CH(CH_3)_2$ (43.0548 Da) for Leu and $^\bullet CH_2CH_3$ (29.0391 Da) for Ile.[27] Because HECD readily produces $z^\bullet$ ions and seldom generates $a^\bullet$ ions, the *w* ions are considerably more abundant than *d* ions. Standard ECD can produce side-chain cleavages, too, but HECD has become the preferred method for distinguishing Xle residues.[30,31] Both HECD and ECD require expensive Fourier transform ion cyclotron resonance instruments, thereby limiting their availability. Whereas there have been efforts to widen ECD availability by modifying benchtop instruments with electromagnetostatic cells, early efforts suffered from relatively poor fragmentation efficiencies,[32,33] and although the efficiencies are now reasonably competitive, the approach still requires multiply charged precursor ions.[20,34–36] Other high-energy fragmentation techniques, like metastable atom-activated dissociation (MAD)[37] and UV photodissociation (UVPD),[38] have also demonstrated an ability to produce side-chain cleavages of Xle residues, and they are applicable to charge states as low as 1+. Of all the techniques, UVPD is closest to widespread adoption, especially because the feature is now commercially available.

Recently, charge transfer dissociation (CTD), which initiates fragmentation through the interaction between a beam of high-energy helium cations and an isolated precursor ion, has been shown to produce radical-driven fragmentation of peptides and oligosaccharides.[39–41] CTD builds on the pioneering work by the separate groups of Zubarev[36] and Schlathölter.[37,38] Both groups explored keV cation–cation reactions of peptides and showed that the high-energy activation produces cleavages of all three types of backbone bonds in peptides in addition to side-chain losses.[42–44] In previous work from our group, fragmentation of Substance P and bradykinin with CTD produced backbone cleavages of all types (*a*/*x*, *b*/*y*, *c*/*z*), as well as some notable side-chain losses.[39,40] However, none of the previous work on CTD focused on the reliability of side-chain losses to discriminate between Xle residues. The present study compares the efficacy of CTD on 1+ and 2+ precursors of model peptides and wild-type peptides to produce either *d* or *w* ions that can discriminate between Xle residues. The results demonstrate that CTD can provide quite reliable differentiation of Xle residues for precursors with a charge state of 1+, which was previously unachievable on a bench-top instrument.

2 | EXPERIMENTAL

2.1 | Instrumentation

A modified Bruker AmaZon mass spectrometer (Bruker Daltonics, Bremen, Germany) was used for the collection of all spectra. The instrument is equipped with a saddle-field fast ion source mounted directly above the ion trap, and UHP helium was used as the CTD reagent gas. The instrument modifications are described in detail elsewhere.[40]

2.2 | Reagents

Model peptides (RGGGGXXGGGGR) were purchased from Pepmic (Pepmic Co. Ltd, Suzhou, China) and reconstituted in a water/methanol/acetic acid mixture (49.5:49.5:1 v/v/v) with a final concentration of 60 ppm. Wild-type peptides (FVIFLDVK, HFSPEDLTVK) were provided by the Julian Laboratory (University of California, Riverside, CA). All peptides were synthesized manually following an accelerated FMOC-protected solid-phase peptide

synthesis protocol.[45] The peptides were reconstituted in a water/acetonitrile/formic acid mixture (49.5:49.5:1 v/v/v) with a final concentration of 100 ppm.

2.3 | Methods

Peptide solutions were introduced to the mass spectrometer using static nanospray with a voltage of −1500 to −1800 V. Singly and doubly charged precursors were isolated with an isolation width of 4 Da. The low-mass cutoff was set to *m/z* 250. CID experiments were performed with an excitation amplitude between 0.5 and 2.0 V with SmartFrag disabled and an activation time of 40 ms. During CTD experiments, the pressure in the main vacuum chamber was maintained between 1.1×10^{-5} and 1.2×10^{-5} mBar. A square-wave voltage of 5–7 kV was applied to the anode of the ion gun to generate an ion beam of 100 ms duration. Precursor ions were stored at a low-mass cutoff of *m/z* 250 during CTD, and product ions were stored for an additional 50 ms after CTD activation to help decrease the chemical background signal from unwanted side reactions. Product ion spectra were collected for 1–2 min in enhanced resolution mode. To negate space charge effects in product ion spectra, any unreacted precursor ions were resonantly ejected using a 3–7 V ejection amplitude before mass acquisition. Negative control experiments verified that the resonance ejection did not produce any collision-induced fragmentation.

2.4 | Data processing

Following conversion to mzML format using MSConvert (http://proteowizard.sourceforge.net/download.html), the spectra were averaged, analyzed and annotated using mMass version 5.5.0.[46–48] The averaged spectra were normalized to the base peak, and automated peak picking was performed with a signal-to-noise threshold of 5.0 and an absolute abundance threshold of 0.3. Annotation of the spectra was performed manually with the aid of Fragmentor (https://sites.google.com/ucr.edu/jlab/software/fragmentor?authuser=0) to predict the masses of peptide fragments.

3 | RESULTS AND DISCUSSION

3.1 | Model peptides

Four model peptides with the sequence RGGGGXXGGGGR, where X is either Leu or Ile, were fragmented using CTD to help establish the propensity for side-chain fragmentation of Xle-containing peptides. Fragmentation of the 1+ precursor via CTD produced a variety of backbone cleavages and surpassed the sequence coverage offered by CID for the same peptide (Figure 1). In addition to *b/y* ions, CTD produced a dominant series of *a/x* ions, similar to observations made with MAD and UVPD fragmentation.[31,38,49] Also, CTD produces several *c/z* ions, which is similar to that of ETD/ECD of the 2+

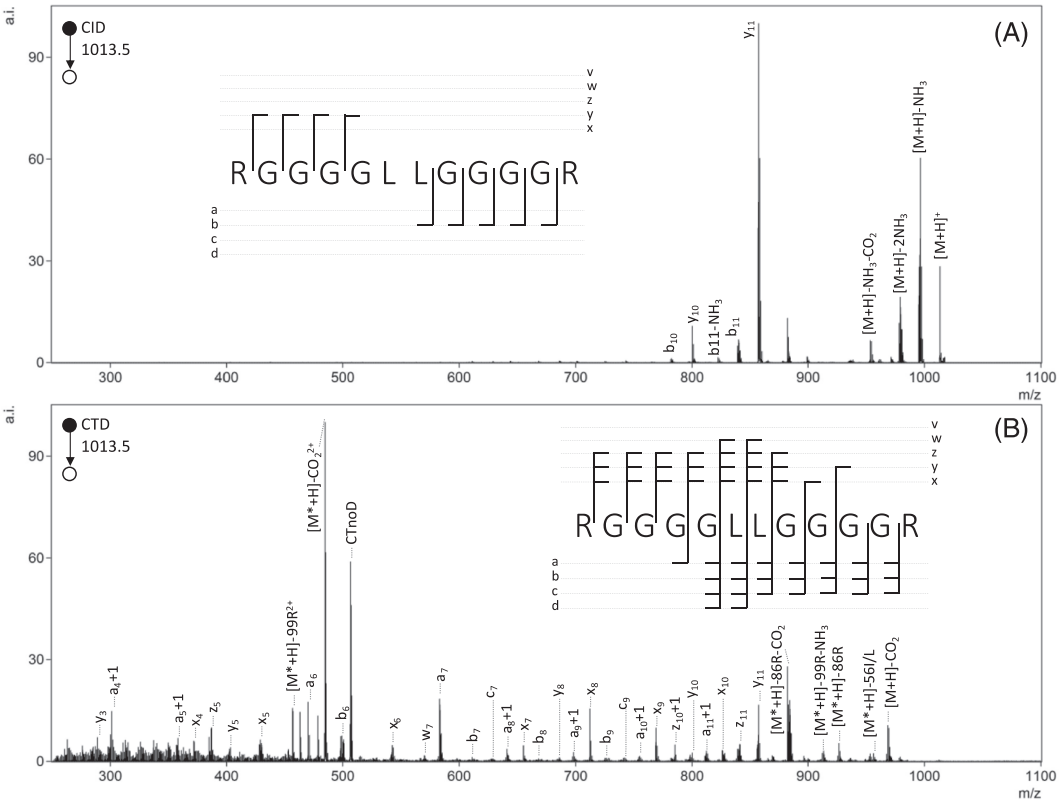

FIGURE 1 (A) CID and (B) CTD spectra of RGGGGLLGGGGR with inset fragmentation maps of the observed backbone cleavages

precursors.[50,51] Some neutral losses are observed in the CTD spectrum, and the most frequently observed neutral loss was for $a_n - NH_3$ ions. Such neutral losses were also observed in previous work on CTD of Substance P.[39]

CTD of the 2+ precursor produces many of the same product ions seen in fragmentation of the singly charged precursor, but the 2+ precursor gave a greater number of ammonia losses. Additionally, many doubly charged product ions are observed in the 2+ spectrum (Figure S1).

Comparison of the CTD spectra of the four isomeric peptides shows that the expected *d* and *w* ions corresponding to the two Xle residues are produced in most, but not all, cases (i.e. 13/16). The abundances of the *d* and *w* ions are often near the signal threshold level, so the ability to average multiple spectra significantly enhances the signal-to-noise level and the ability to identify these low-abundance ions. Such averaging might be problematic in situations where ion signals are more transient, such as with on-line coupling of CTD with high-performance liquid chromatography.

Regarding CTD of the 1+ precursor of RGGGG**LL**GGGGR and RGGGG**LI**GGGGR, both peptides produced a d_6 ion at *m/z* 428.1 (Figure 2B), which is consistent with a side-chain loss of 43 Da from the a_6 ion and is therefore diagnostic for Leu at position 6. Similarly, the peptides RGGGG**IL**GGGGR and RGGGG**II**GGGGR produced d_6 ions at *m/z* 442.1, which are consistent with a side-chain loss of 29 Da from their respective a_6 ions and are diagnostic for Ile at position 6 (Figure 2C).

To discriminate Leu from Ile in the seventh position, w_6 diagnostic ions should be observed at *m/z* 457.1 or *m/z* 471.2, respectively. As seen in Figure 3B, the w_6 ion at *m/z* 457.1 overlaps with the ^{13}C isotopic envelope of the $M - 99R^{2+}$ species, which is a characteristic side-chain loss for arginine.[34] For all four peptides, the isotope envelope accompanying the peak at *m/z* 457.1 includes a ^{13}C isotope peak at *m/z* 457.6, which confirms the presence of the 2+ product ion but complicates the relative contribution of the w_6 ion at *m/z* 457.1. The relative abundance of the $M - 99R^{2+}$ peak at *m/z* 457.1 differs considerably depending on the peptide sequence. For peptides with Leu in the seventh position, the abundance of the peak at *m/z* 457.1 is approximately double that of peptides with Ile in the seventh position. The abundance of a related side-chain fragment of arginine at $M - 86R^{2+}$ also correlates with the abundance of the $M - 99R^{2+}$ peak.

The two peptides with Ile in position 7 also produce CTD product ion spectra with a background or interference peak at *m/z* 457.1. To help assess the significance of the peak abundance at *m/z* 457.1, we therefore assessed the abundance of the w_6 ion relative to the z_6 ion from which it derives, and the results are described in more detail in section 3.2. The w_6 ion at *m/z* 471.2 is diagnostic for Ile in the seventh position, and this fragment overlaps with the possible $a_6 + 1$ ion (Figure 3C). However, the relative abundance of the $z_6 - 29$ peak is similar for all four peptide sequences, so the presence of a w_6 ion for Ile at position 7 cannot be confirmed without high mass accuracy.

Fragmentation of the 2+ precursors also produced *d* and *w* ions, which are complementary to those observed in the 1+ spectra. A d_6

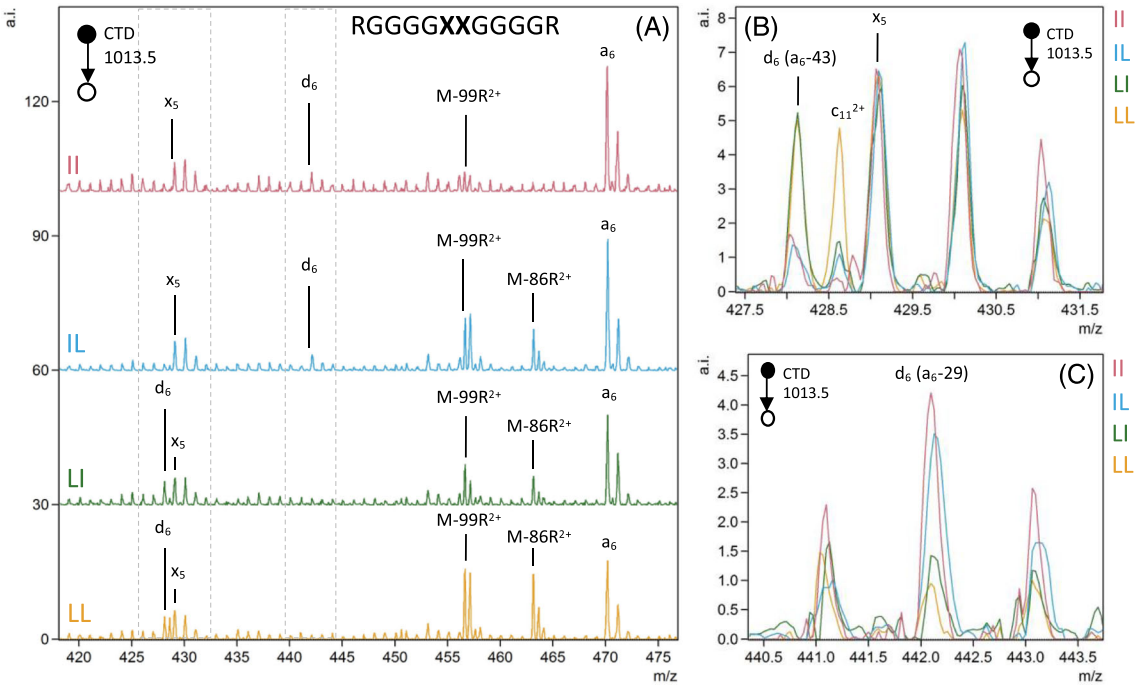

FIGURE 2 (A) CTD fragmentation of singly charged precursors produces *d* ions for each of the four model peptide sequences (RGGGG**LL**GGGGR in orange, RGGGG**LI**GGGGR in green, RGGGG**IL**GGGGR in blue, RGGGG**II**GGGGR in pink). (B) Magnification of the region for the d_6 ion that is diagnostic for Leu in the sixth position. (C) Magnification of the region for the d_6 ion that is diagnostic for Ile in the sixth position [Color figure can be viewed at wileyonlinelibrary.com]

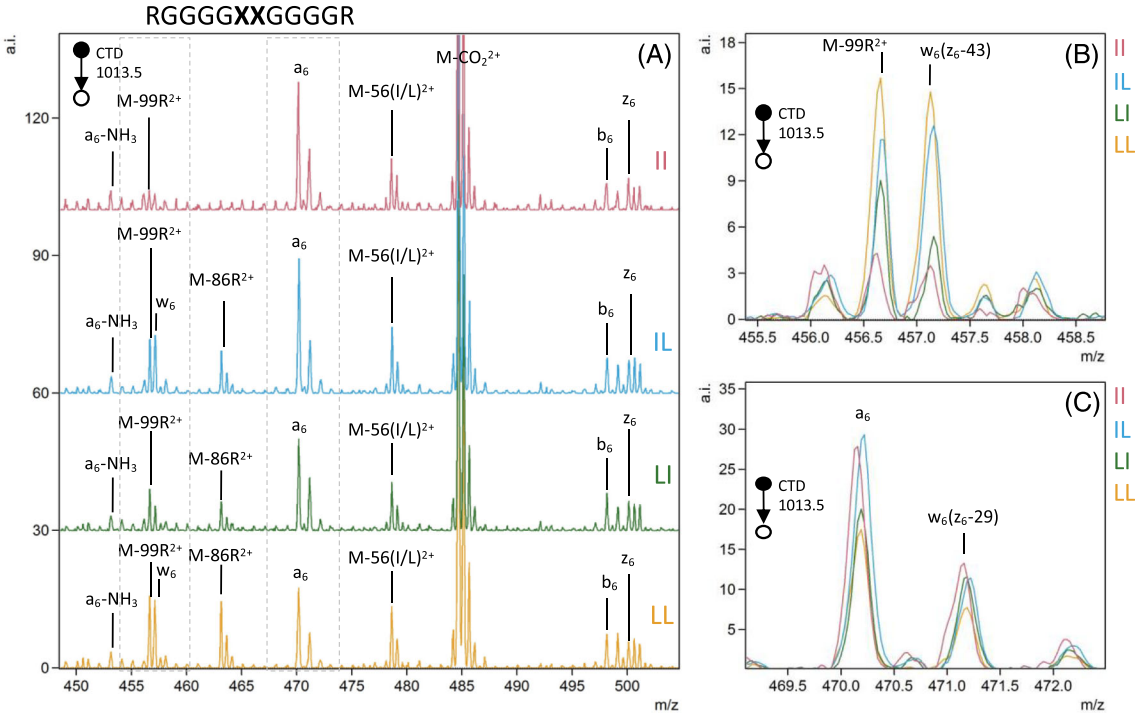

FIGURE 3 (A) CTD fragmentation of singly charged precursors produces *w* ions for each of the four model peptide sequences (RGGGG**LL**GGGGR in orange, RGGGG**LI**GGGGR in green, RGGGG**IL**GGGGR in blue, RGGGG**II**GGGGR in pink). (B) Magnification of the w_6 ion diagnostic for Leu in the seventh position. Though overlapping with the isotopic envelope of M − 99R^{2+}, the peak at *m*/*z* 457.1 is more abundant for RGGGG**LL**GGGGR and RGGGG**IL**GGGGR than for the other sequences. (C) Magnification of the w_6 ion diagnostic for Ile in the seventh position shows no noticeable difference in the relative abundance of the ion at *m*/*z* 471.2 [Color figure can be viewed at wileyonlinelibrary.com]

ion at *m*/*z* 428.1, which is diagnostic for Leu, appears to be more abundant for RGGGG**LL**GGGGR than for the other peptides, but this peak is generally of too low an abundance to be a reliable indicator of the amino acid identity in the sixth position. A d_6 ion diagnostic for Ile in the sixth position at *m*/*z* 442.1 is observed for both RGGGG**II**GGGGR and RGGGG**IL**GGGGR (Figure 4C). However, the relative abundances of the expected and decoy (not expected) peaks do not provide the level of confidence one requires for *de novo* sequencing, so this *d* ion is not as reliable as for the 1+ precursor. The reliability of *d* ions in the 1+ spectra compared to the 2+ spectra presumably derives from the fact that *a* and *d* ions are typically more abundant in CTD spectra of 1+ peptides.[34]

The M − 99R^{2+} ion observed in the 1+ spectra is absent in the 2+ spectra, which allows for more confident assignment of the w_6 ion at *m*/*z* 457.1 (Figure 5B). Although the ion at *m*/*z* 471.2 still overlaps with the isotopic envelope of the a_6 ion in the 2+ spectra, the spectra show significant differences in the relative abundances among the four peptides. For the peptides with Ile in the seventh position, the abundance of the w_6 peak at *m*/*z* 471.2 is approximately equal to the abundance of the a_6 ion. In contrast, for peptides with Leu in the seventh position, the decoy peak at *m*/*z* 471.2 is half the abundance of the a_6 peak (Figure 5C).

Information gathered from both the CTD spectra of 1+ and 2+ precursors of the different peptides suggests that discrimination between Leu and Ile is possible through both d_6 and w_6 ions, which originate from cleavages between the two Xle residues. Other potential diagnostic ions for Xle differentiation, such as d_7 and w_7 ions, were also investigated, but the abundances were either too small or too variable to be reliable. In the four model peptides, cleavages between the glycine (Gly) and Xle residues resulted in low-abundance z_7 and w_7 ions. In contrast, N-terminal a_7 ions—which also form between Gly-Xle residues—were readily abundant for all four model peptides. However, the abundances of the corresponding d_7 ions were still insufficient to permit confident assignment of the Xle isomers. For these reasons, Xle isomers in the seventh position of the model peptides were therefore only reliably accessed from the C-terminus and through the w_6 fragments.

3.2 | Diagnostic *d*/*a* and *w*/*z* abundance ratios for Xle identification

As described above, the abundance of the diagnostic *d* and *w* ions of the Xle residues is often sufficiently small as to create ambiguity about their relevance. To create a more objective assessment of the presence or significance of peaks that could be attributed to *d* or *w* ions, we developed a simple method to compare the abundance ratios of *d* and *w* ions to the corresponding *a* and *z* ions from which they derive. In the proposed approach, if the corresponding *a* or *z* ion is below an arbitrary threshold, the abundance of a different—

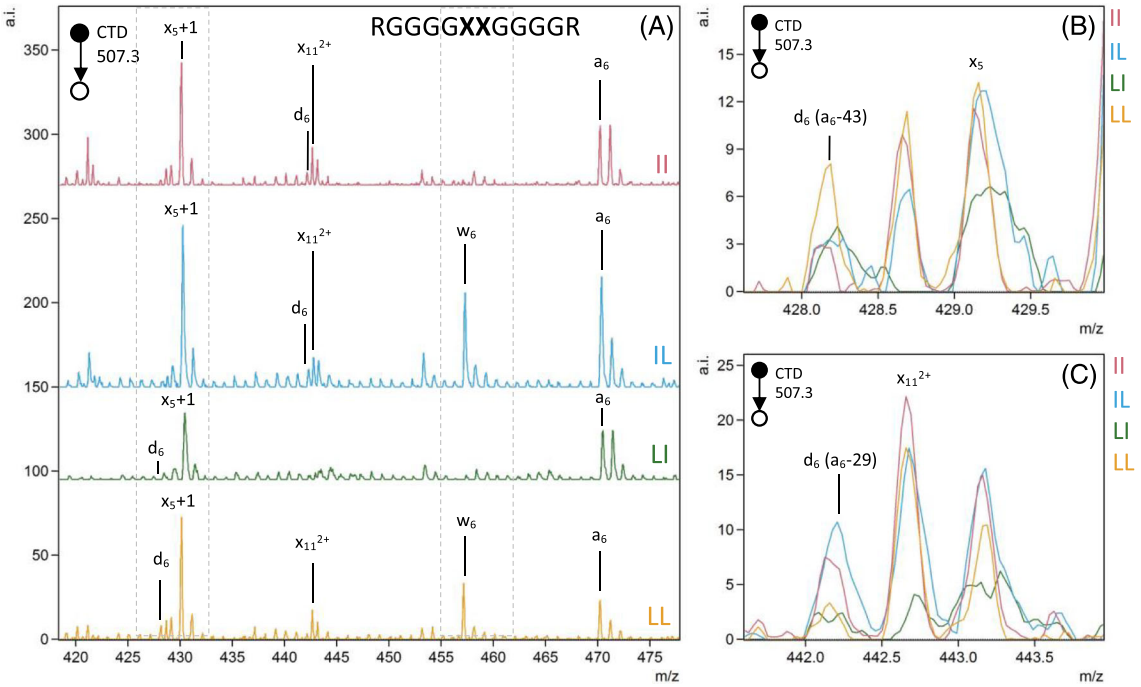

FIGURE 4 (A) CTD fragmentation of doubly charged precursors produces *d* ions for each of the four model peptide sequences (RGGGG**LL**GGGGR in orange, RGGGG**LI**GGGGR in green, RGGGG**IL**GGGGR in blue, RGGGG**II**GGGGR in pink). (B) Magnification of the d_6 ion diagnostic for Leu in the sixth position. The peak at *m/z* 428.1 is somewhat more abundant for RGGGG**LL**GGGGR than for the other peptides but does not appear to be a reliable indicator of Leu in the sixth position. (C) Magnification of the d_6 ion diagnostic for Ile in the sixth position shows a greater abundance for RGGGG**II**GGGGR and RGGGG**IL**GGGGR over peptides without Ile in the sixth position [Color figure can be viewed at wileyonlinelibrary.com]

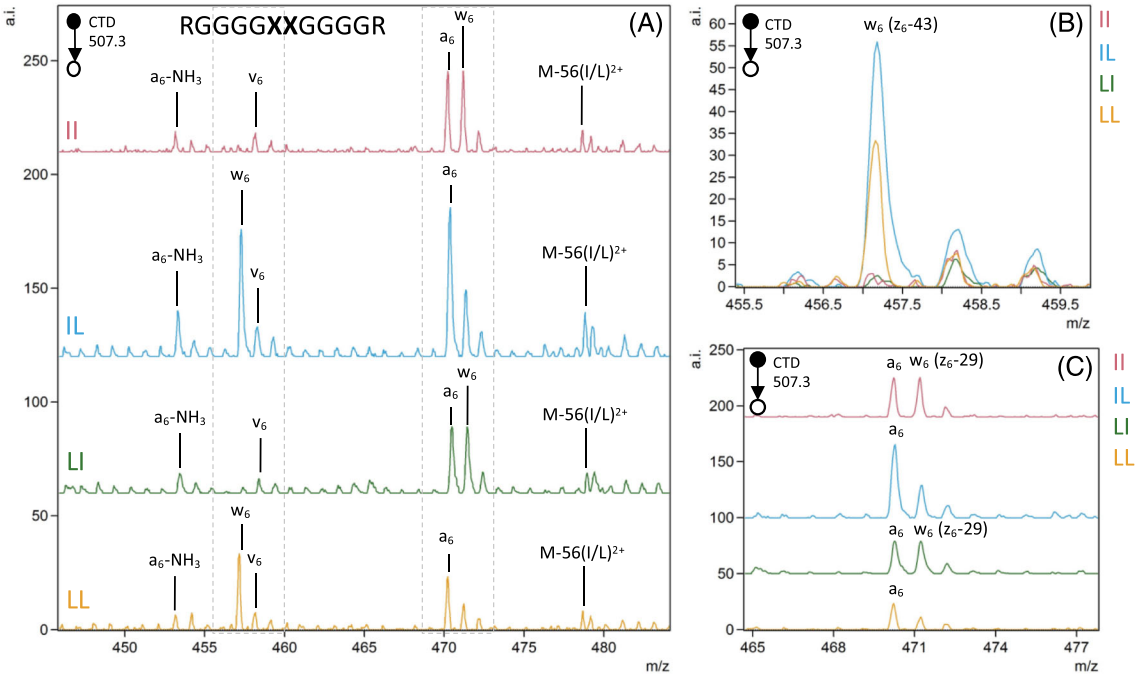

FIGURE 5 (A) CTD fragmentation of doubly charged precursors produces *w* ions for each of the four model peptide sequences (RGGGG**LL**GGGGR in orange, RGGGG**LI**GGGGR in green, RGGGG**IL**GGGGR in blue, RGGGG**II**GGGGR in pink). (B) Magnification of the w_6 ion diagnostic for Leu in the seventh position. (C) Magnification of the w_6 ion diagnostic for Ile in the seventh position. Though overlapping with the isotopic envelope of a_6, the peak at *m/z* 471.2 is more abundant for RGGGG**II**GGGGR and RGGGG**LI**GGGGR than for the other sequences [Color figure can be viewed at wileyonlinelibrary.com]

but structurally and spectrally related—ion is used as a comparison to the selected *w* ion. For example, most of the z_6 ions for the 2+ model peptides fell below the threshold for peak identification, so the corresponding a_6 ion was used to compare abundance ratios, as shown in Figure S2B. The *d*/*a* or *w*/*z* abundance ratios are then calculated for both the expected fragments—such as the loss of 43 Da for Leu, if a Leu is present—and a decoy fragment, such as the loss of 29 Da, if Leu is present. Ideally, the decoy fragment should not be observed at all, but most of the CTD spectra contain some level of background signal or isobaric interference at the decoy position, hence the need for *d*/*a* and *w*/*z* abundance comparisons.

For the four model peptides, the expected fragments had a significantly higher abundance ratio (*t*-test, $p < 0.05$, power > 0.9) than the hypothetical decoy in 13 of the 16 cases (81%). Eight comparisons for the *d*/*a* ion pairs are shown in Figure 6. The results of the *w*/*z* ion pairs are shown in Figure S2. As an example, the w_6 fragment for RGGGG**II**GGGGR^{1+} has average abundance ratios relative to the z_6 fragment of 2.12 and 0.61 for the expected and decoy peaks, respectively. Using a ratio of 1 as a threshold would accurately identify Ile in the sixth position. In a more challenging case, like the w_6 ion for RGGGG**IL**GGGGR^{1+}, the average abundance ratios for w_6/z_6 ion pairs were 1.79 and 1.58, respectively, for the expected and decoy fragments. The lack of significant difference between the expected and decoy peaks in this case makes it impossible to distinguish the Xle residues. Our findings are consistent with prior work in that when an Xle residue is suspected, the abundance of the *d* or *w* ion for the expected side-chain loss is significantly greater than the abundance of the decoy loss.[27] However, the *d* or *w* ions are only reliably present about 80% of the time in the model peptides, so the Xle residues are sometimes not resolvable.

The three exceptions that did not show significant differences between expected and decoy ion pairs were the d_6 ion for RGGGG**II**GGGGR^{1+}, the w_6 ion for RGGGG**IL**GGGGR^{1+} (Figure S2) and the d_6 ion for RGGGG**LI**GGGGR^{2+}. The d_6 ions for RGGGG**II**GGGGR^{1+} and RGGGG**LI**GGGGR^{2+} were too low in abundance or too variable to be significantly different from the decoy ion. For RGGGG**IL**GGGGR^{2+}, the decoy ion of w_6 is isobaric with a ^{13}C ion of a_6, which negatively impacted the abundance ratio. Except for these three cases, the expected fragment had a reliably greater abundance ratio than the hypothetical decoy. The results are summarized in a box-and-whisker plot in Figure 6.

Unfortunately, the d_6/a_6 ratios are not of similar enough magnitudes for the four peptides to permit a universal threshold with which to discriminate between Xle residues. For example, for the 1+ precursor in Figure 6A, a threshold d_6/a_6 value of 0.15 would

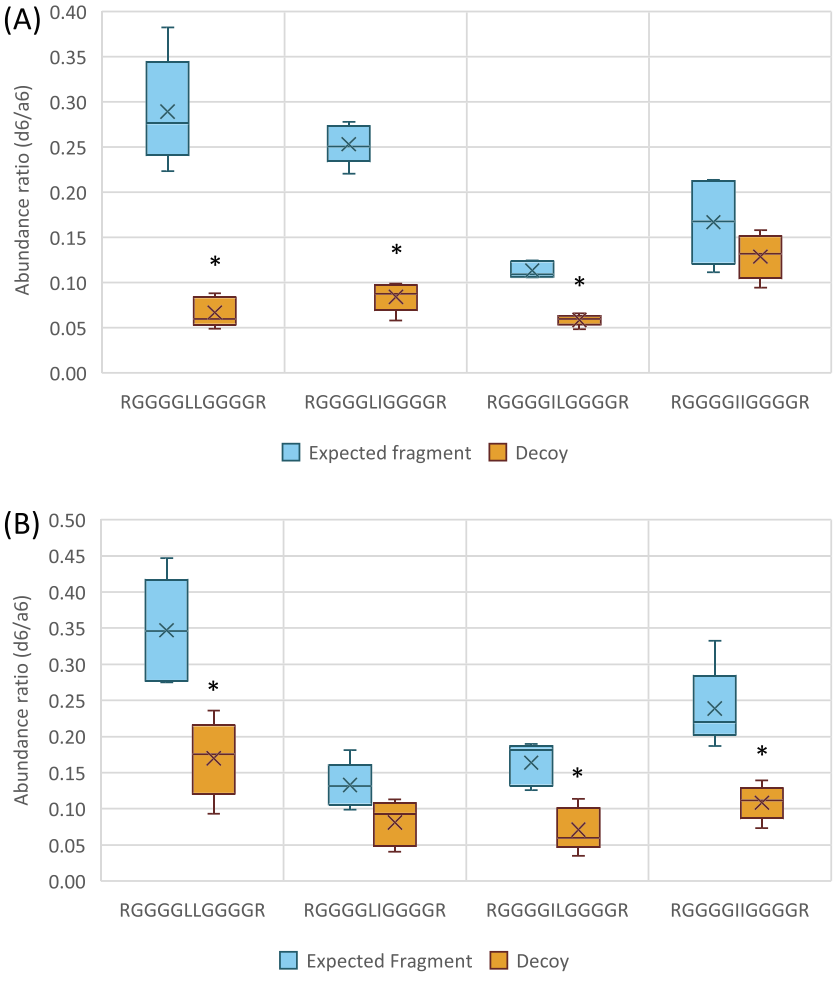

FIGURE 6 Abundance ratios for expected d_6 fragments (light blue) and decoys (orange) for 1+ (A) and 2+ (B) model peptides. Asterisks indicate pairs that are significantly different (*t*-test, $p < 0.05$, power > 0.9, $n = 5$) [Color figure can be viewed at wileyonlinelibrary.com]

successfully discriminate three of the four Xle residues in the sixth position, but a threshold of 0.1 would be required to identify Ile in the sixth position for RGGGG**II**GGGGR^{1+}. For the 2+ precursors, a threshold of 0.2 would correctly identify Leu and Ile in RGGGG**LL**GGGGR^{2+} and RGGGG**II**GGGGR^{2+}, respectively, but a lower threshold of 0.1 would be required to resolve the Xle residues

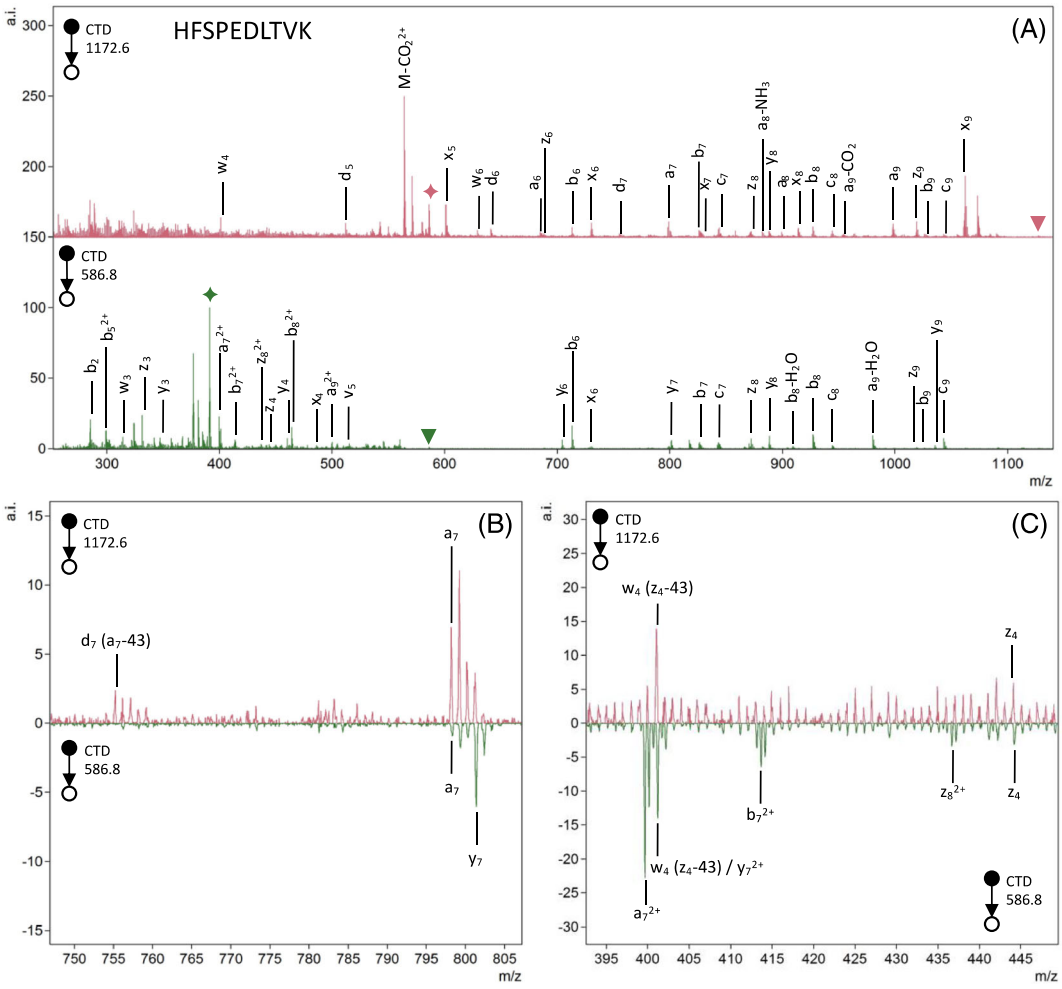

FIGURE 7 (A) Stacked CTD spectra of HFSPEDLTVK with triangles representing the resonantly ejected precursor and diamonds representing the CTnoD product. (B) Head-to-tail magnification of the a_7 → d_7 ion with 1+ precursor in pink and 2+ precursor in green. (C) Head-to-tail magnification of the z_4 → w_4 ion. In the 2+ spectra, the w_4 ion falls at the same m/z value as the y_7^{2+} ion [Color figure can be viewed at wileyonlinelibrary.com]

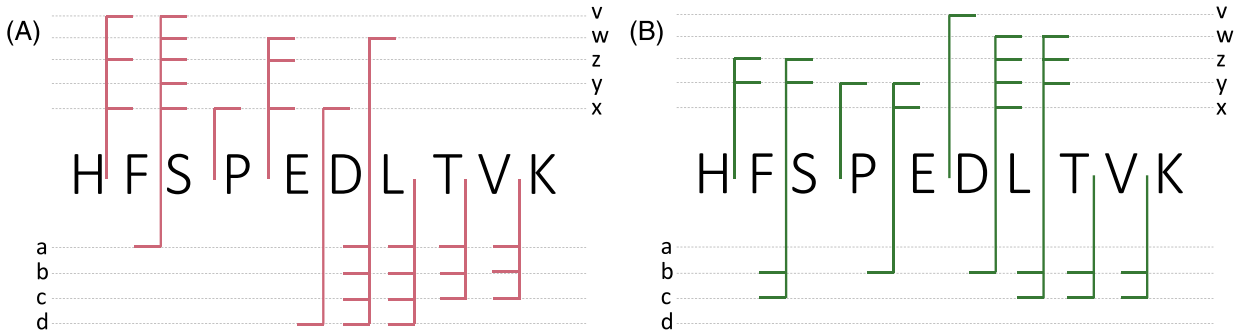

FIGURE 8 Backbone cleavages from CTD of the (A) 1+ precursor and the (B) 2+ precursor of HFSPEDLTVK [Color figure can be viewed at wileyonlinelibrary.com]

in RGGGG**IL**GGGGR^{2+} and RGGGG**LI**GGGGR^{2+}. For these reasons, the use of a general, data-independent threshold of *ca* 0.2 for *de novo* peptide sequencing probably only confidently assigns about 50% of the Xle residues. Such discrimination could still be valuable in certain applications.

3.3 | Wild-type peptides

Having established that CTD can produce *d* and *w* ions for Xle residues approximately 80% of the time in the model peptides, we then investigated two additional wild-type peptides that had more complex sequences. The first peptide, HFSPEDLTVK, from the human alpha-crystallin A chain, has a single Leu residue at position 7. CTD spectra of the 1+ and 2+ precursors are shown in Figure 7. Like the model peptides, CTD of the singly charged precursor produced an abundant array of *a*/*x*, *b*/*y*, *c*/*z* and *d*/*w* ions, but CTD of the doubly charged precursor produced less-abundant *a*/*x* ions. These findings are consistent with previous work on CTD of other peptides.[34] Some additional side-chain losses, such as *v* ions, were also observed in the CTD spectra of both 1+ and 2+ precursors. Fragment ion maps in Figures 8 and 9 help show the observed fragments.

Reliable *d* and *w* ions diagnostic for Leu can be identified in the 1+ spectra (Figures 7B and 7C). Notably, the w_4 ion abundance exceeds that of the z_4 ion from which it derives, suggesting CTD can achieve similar energies or follows fragmentation mechanisms similar to those of HECD. Energy-dependent studies of the formation of *w* ions with HECD showed that the relative abundance of *w* ions increases with higher electron energies.[52] Many secondary ions reported with HECD are about one-third to one-half the abundance of the *z* ions from which they derive, but at higher energies, the *w* ion abundance can match or exceed the abundance of its corresponding *z* ion.[27,28,52] The 2+ precursor did not produce any *a* ions, which probably explains why no *d* ions were observed either. In the CTD spectrum of the 2+ precursor, the 1+ product ion at *m*/*z* 401.2 has an ambiguous identity because the *w* ion for Leu overlaps with a y_7^{2+} ion (Figure 7C). We know the y_7^{2+} ion is present because of the spacing of the isotope envelope is 0.5 Da.

In addition to the side-chain losses for Leu, side-chain losses are observed for other amino acids in the sequence, too. In the singly charged species (Figure 8A), *w* ions are observed for glutamate and serine, and *d* ions are observed for glutamate and aspartate. At *m*/*z* 856.4 and *m*/*z* 943.5, *v* ions are observed for serine and phenylalanine, respectively. In the doubly charged species (Figure 8B), a *w* ion is observed for threonine and a *v* ion is observed for aspartate. These fragments suggest that CTD may be able to differentiate other isomeric amino acids through these unique side-chain losses.

The second wild-type peptide, FVIFLDVK, has both a Leu and an Ile present in the sequence. Many types of backbone cleavages are present in the CTD spectra of the 1+ and 2+ precursors, but *a* and *d* ions are again absent in the 2+ spectra (Figures 9 and 10). For the 1+ precursor, a low-abundance d_5 ion, diagnostic for Leu, is questionable at *m*/*z* 549.2, and the d_3 ion for Ile cannot be identified because it falls in the low-mass region of the spectrum that contains high chemical background (Figure 10B). However, a reliable w_4 ion at *m*/*z* 415.2 is present in the spectra from both precursors, and the w_4 fragment is slightly more abundant than the corresponding z_4 ion in both cases (Figure 10C). A w_6 ion, diagnostic for Ile, is also present in both spectra. Notably, a low-abundance w_6b ion is present in the 1+ spectra of FVIFLDVK (Figure 10D), which is a loss of −15 Da from the corresponding *z* ion. Since Ile has a forked side chain, there is a possibility for a loss of -CH_3 from the corresponding *z* ion, which generates a w_nb ion. However, a loss of -CH_3 from Ile is generally unfavored, so this particular type of ion is rarely reported for Ile.[13] Other side-chain losses (*w*/*d* and *v* ions) are also observed for phenylalanine, valine and aspartic acid (Figure 9).

Diagnostic *d*/*a* and *w*/*z* abundance ratios for Xle identification were calculated for both wild-type peptides. In each instance, the expected fragment ratio was significantly different from the decoy ratio (Figures S3 and S4). This provides an added level of confidence in identification of the Xle residues within the selected peptides.

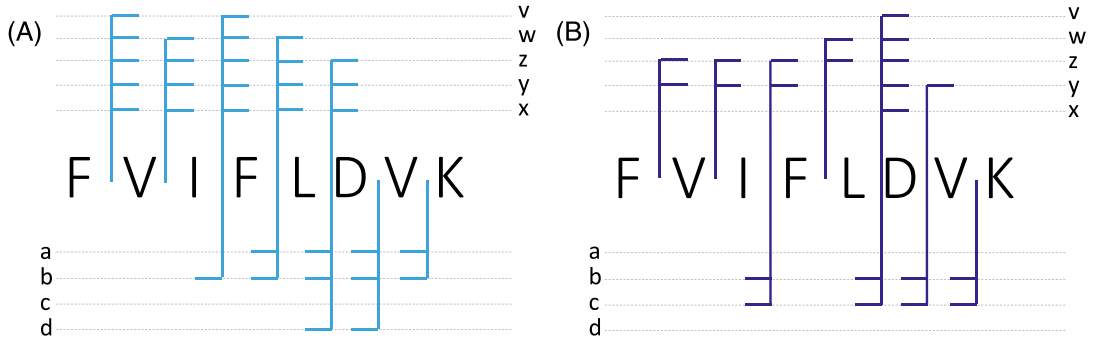

FIGURE 9 Backbone cleavages produced by CTD of the (A) 1+ precursor and the (B) 2+ precursor of FVIFLDVK [Color figure can be viewed at wileyonlinelibrary.com]

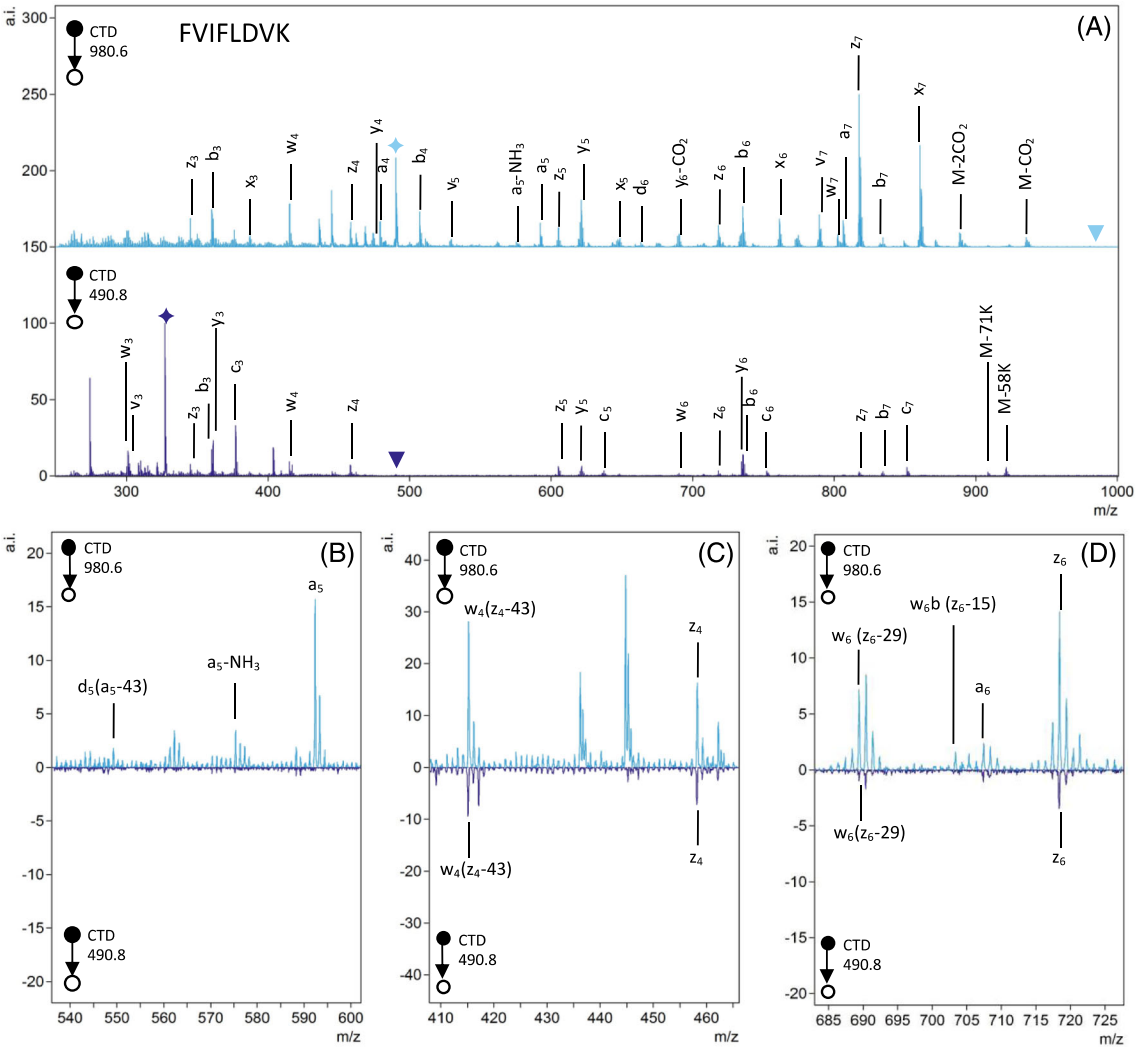

FIGURE 10 (A) Stacked CTD spectra of FVIFLDVK with triangles representing the resonantly ejected precursor and diamonds representing the CTnoD product. (B) Head-to-tail magnification of the a_5 → d_5 ion, diagnostic for Leu, with 1+ spectra in blue and 2+ spectra in purple. Neither a_5 nor d_5 ions are observed in the 2+ spectra. (C) Head-to-tail magnification of the z_4 → w_4 ion, which is characteristic of Leu. (D) Head-to-tail magnification of the z_6 → w_6 ion, which is diagnostic for Ile. A w_6b ion is also observed in the 1+ spectra [Color figure can be viewed at wileyonlinelibrary.com]

4 | CONCLUSIONS

For the fragmentation of model and wild-type peptides, CTD provides fragment ion types that are comparable with those of other high-energy techniques, like ECD, ETD and UVPD. Especially for the 1+ precursor, CTD produces quite reliable *a* and *x* ions, which are commonly observed with UVPD of 1+ precursors. For the 2+ precursors, CTD provided less-abundant *a* and *d* ions, but more-abundant *c* and *z* ions, which are generally more abundant in ECD and ETD spectra of multiply charged precursors.

Important side-chain cleavages are also observed with CTD, marking another similarity to other dissociation methods like EtHCD[21,23] and HECD—which reliably produces *w* ions for multiply charged peptides[13,27]—and 157 nm UVPD, which produces both *d* and *w* ions for singly charged peptides.[53,54] CTD produces both *d* and *w* ions from either 1+ or 2+ charged precursors on a three-dimensional ion trap instrument, giving a slight advantage over other techniques that require multiply charged precursors and more expensive instruments, like high-field Fourier transform ion cyclotron resonance mass spectrometers. Reliable differentiation between Leu and Ile was possible through the generation of *d*/*w* ions that are diagnostic for Leu or Ile, although differentiation was not always unambiguous. Fragments such as *d* and *w* ions were observed for about a third of the amino acid residues in each peptide, and these results indicate that CTD can contribute to the differentiation between other isomeric amino acids, such as through *d* and *w* ions for aspartic acid/isoaspartic acid and *d* and *w* ions for valine/norvaline.

ACKNOWLEDGMENTS

The authors thank Yana A. Lyon for synthesizing the FVIFLDVK peptide used in this study. This work was supported by the National Science Foundation (NSF) (CHE-1710376 for GPJ and HCE-1904577 for RRJ) and the National Institutes of Health (NIH) (1R01GM114494-01 for GPJ). The opinions, findings and conclusions or recommendations expressed in this publication are those of the author(s) and do not necessarily reflect the views of NSF or NIH.

PEER REVIEW

The peer review history for this article is available at https://publons.com/publon/10.1002/rcm.9246.

DATA AVAILABILITY STATEMENT

The data that support the findings of this study are available from the corresponding author upon reasonable request.

ORCID

Glen P. Jackson https://orcid.org/0000-0003-0803-6254

REFERENCES

1. Bagal D, Kast E, Cao P. Rapid distinction of leucine and isoleucine in monoclonal antibodies using Nanoflow LCMSn. *Anal Chem*. 2017;89(1):720-727. doi:10.1021/acs.analchem.6b03261
2. Coronavirus (COVID-19) Update: FDA authorizes monoclonal antibodies for treatment of COVID-19. FDA. https://www.fda.gov/news-events/press-announcements/coronavirus-covid-19-update-fda-authorizes-monoclonal-antibodies-treatment-covid-19-0. Accessed February 11, 2021.
3. Waldmann TA. Immunotherapy: Past, present and future. *Nat Med*. 2003;9(3):269-277. doi:10.1038/nm0303-269
4. Bandeira N, Pham V, Pevzner P, Arnott D, Lill JR. Automated de novo protein sequencing of monoclonal antibodies. *Nat Biotechnol*. 2008;26(12):1336-1338. doi:10.1038/nbt1208-1336
5. Tao WA, Wu L, Cooks RG. Differentiation and quantitation of isomeric dipeptides by low-energy dissociation of copper(II)-bound complexes. *J Am Soc Mass Spectrom*. 2001;12(5):490-496.
6. Seymour JL, Turecek F. Distinction and quantitation of leucine-isoleucine isomers and lysine-glutamine isobars by electrospray ionization tandem mass spectrometry (MSn,n = 2, 3) of copper(II)-diimine complexes. *J Mass Spectrom*. 2000;35(4):566-571.
7. Poston CN, Higgs RE, You J, et al. A quantitative tool to distinguish isobaric leucine and isoleucine residues for mass spectrometry-based de novo monoclonal antibody sequencing. *J Am Soc Mass Spectrom*. 2014;25(7):1228-1236. doi:10.1007/s13361-014-0892-1
8. Armirotti A, Millo E, Damonte G. How to discriminate between leucine and isoleucine by low energy ESI-TRAP MSn. *J Am Soc Mass Spectrom*. 2007;18(1):57-63. doi:10.1016/j.jasms.2006.08.011
9. Maibom-Thomsen S, Heissel S, Mørtz E, Højrup P, Bunkenborg J. Discrimination of isoleucine and leucine by dimethylation-assisted MS3. *Anal Chem*. 2018;90(15):9055-9059. doi:10.1021/acs.analchem.8b01375
10. Nakamura T, Nagaki H, Ohki Y, Kinoshita T. Differentiation of leucine and isoleucine residues in peptides by consecutive reaction mass spectrometry. *Anal Chem*. 1990;62(3):311-313.
11. Biemann K, Martin SA. Mass spectrometric determination of the amino acid sequence of peptides and proteins. *Mass Spectrom Rev*. 1987;6(1):1-76.
12. Johnson RS, Martin SA, Biemann K, Stults JT, Watson JT. Novel fragmentation process of peptides by collision-induced decomposition in a tandem mass spectrometer: Differentiation of leucine and isoleucine. *Anal Chem*. 1987;59(21):2621-2625. doi:10.1021/ac00148a019
13. Savitski MM, Nielsen ML, Zubarev RA. Side-chain losses in electron capture dissociation to improve peptide identification. *Anal Chem*. 2007;79(6):2296-2302. doi:10.1021/ac0619332
14. Fung YME, Chan TWD. Experimental and theoretical investigations of the loss of amino acid side chains in electron capture dissociation of model peptides. *J Am Soc Mass Spectrom*. 2005;16(9):1523-1535. doi:10.1016/j.jasms.2005.05.001
15. Asakawa D. Ultraviolet-laser-induced electron transfer from peptides to an oxidizing matrix: Study of the first step of MALDI in-source decay mass spectrometry. *J Am Soc Mass Spectrom*. 2020;31(9):1918-1926. doi:10.1021/jasms.0c00186
16. Asakawa D. Cooperative dissociation of peptide backbones and side-chains during matrix-assisted laser desorption/ionization in-source decay mediated by hydrogen abstraction. *J Mass Spectrom*. 2021;56(4):1-11. doi:10.1002/jms.4530
17. van Agthoven MA, Lynch AM, Morgan TE, et al. Can two-dimensional IR-ECD mass spectrometry improve peptide de novo sequencing? *Anal Chem*. 2018;90(5):3496-3504. doi:10.1021/acs.analchem.7b05324
18. Xiao Y, Vecchi MM, Wen D. Distinguishing between leucine and isoleucine by integrated LC−MS analysis using an Orbitrap fusion mass spectrometer. *Anal Chem*. 2016;88(21):10757-10766. doi:10.1021/acs.analchem.6b03409
19. Gupta K, Kumar M, Chandrashekara K, Krishnan KS, Balaram P. Combined electron transfer dissociation-collision-induced dissociation fragmentation in the mass spectrometric distinction of leucine, isoleucine, and hydroxyproline residues in peptide natural products. *J Proteome Res*. 2012;11(2):515-522. doi:10.1021/pr200091v
20. Shaw JB, Malhan N, Vasil'ev YV, et al. Sequencing grade tandem mass spectrometry for top-down proteomics using hybrid electron capture dissociation methods in a benchtop Orbitrap mass spectrometer. *Anal Chem*. 2018;90(18):10819-10827. doi:10.1021/acs.analchem.8b01901
21. Zhokhov SS, Kovalyov SV, Samgina TY, Lebedev AT. An EThcD-based method for discrimination of leucine and isoleucine residues in tryptic peptides. *J Am Soc Mass Spectrom*. 2017;28(8):1600-1611. doi:10.1007/s13361-017-1674-3
22. Lebedev AT, Damoc E, Makarov AA, Samgina TY. Discrimination of leucine and isoleucine in peptides sequencing with Orbitrap fusion mass spectrometer. *Anal Chem*. 2014;86(14):7017-7022. doi:10.1021/ac501200h
23. Samgina TY, Kovalev SV, Tolpina MD, Trebse P, Torkar G, Lebedev AT. EThcD discrimination of isomeric leucine/isoleucine residues in sequencing of the intact skin frog peptides with intramolecular disulfide bond. *J Am Soc Mass Spectrom*. 2018;29(5):842-852. doi:10.1007/s13361-017-1857-y
24. Asakawa D, Smargiasso N, De Pauw E. Discrimination of isobaric Leu/Ile residues by MALDI in-source decay mass spectrometry. *J Am Soc Mass Spectrom*. 2013;24(2):297-300. doi:10.1007/s13361-012-0523-7
25. Soltwisch J, Dreisewerd K. Discrimination of isobaric leucine and isoleucine residues and analysis of post-translational modifications in peptides by MALDI in-source decay mass spectrometry combined with collisional cooling. *Anal Chem*. 2010;82(13):5628-5635. doi:10.1021/ac1006014
26. Kjeldsen F, Haselmann KF, Budnik BA, Jensen F, Zubarev RA. Dissociative capture of hot (3-13 eV) electrons by polypeptide polycations: An efficient process accompanied by secondary fragmentation. *Chem Phys Lett*. 2002;356(3-4):201-206.
27. Kjeldsen F, Haselmann KF, Sørensen ES, Zubarev RA. Distinguishing of Ile/Leu amino acid residues in the PP3 protein by (hot) electron

capture dissociation in Fourier transform ion cyclotron resonance mass spectrometry. *Anal Chem*. 2003;75(6):1267-1274. doi:10.1021/ac020422m
28. Liang Z, Yu X, Zhong W. Peptide sequence influence on the differentiation of valine and norvaline by hot electron capture dissociation. *Anal Chem*. 2019;91(7):4381-4387. doi:10.1021/acs.analchem.8b04808
29. Williams JP, Creese AJ, Roper DR, Green BN, Cooper HJ. Hot electron capture dissociation distinguishes leucine from isoleucine in a novel hemoglobin variant, Hb askew, B54(D5)Val→Ile. *J Am Soc Mass Spectrom*. 2009;20(9):1707-1713. doi:10.1016/j.jasms.2009.05.002
30. Cooper HJ, Hudgins RR, Håkansson K, Marshall AG. Secondary fragmentation of linear peptides in electron capture dissociation. *Int J Mass Spectrom*. 2003;228(2-3):723-728. doi:10.1016/S1387-3806(03)00202-1
31. Cooper HJ, Hudgins RR, Håkansson K, Marshall AG. Characterization of amino acid side chain losses in electron capture dissociation. *J Am Soc Mass Spectrom*. 2002;13(3):241-249. doi:10.1016/S1044-0305(01)00357-9
32. Voinov VG, Bennett SE, Barofsky DF. Electron-induced dissociation of peptides in a triple quadrupole mass spectrometer retrofitted with an electromagnetostatic cell. *J Am Soc Mass Spectrom*. 2015;26(5):752-761. doi:10.1007/s13361-014-1074-x
33. Voinov VG, Deinzer ML, Barofsky DF. Electron capture dissociation in a linear radiofrequency-free magnetic cell. *Rapid Commun Mass Spectrom*. 2008;22(19):3087-3088. doi:10.1002/rcm.3709
34. Williams JP, Morrison LJ, Brown JM, Beckman JS, Voinov VG, Lermyte F. Top-down characterization of denatured proteins and native protein complexes using electron capture dissociation implemented within a modified ion mobility-mass spectrometer. *Anal Chem*. 2020;92(5):3674-3681. doi:10.1021/acs.analchem.9b04763
35. Gadkari VV, Ramírez CR, Vallejo DD, Kurulugama RT, Fjeldsted JC, Ruotolo BT. Enhanced collision induced unfolding and electron capture dissociation of native-like protein ions. *Anal Chem*. 2020;92(23):15489-15496. doi:10.1021/acs.analchem.0c03372
36. Beckman JS, Voinov VG, Hare M, et al. Improved protein and PTM characterization with a practical electron-based fragmentation on Q-TOF instruments. *J Am Soc Mass Spectrom*. 2021;32(8):2081-2091. doi:10.1021/jasms.0c00482
37. Cook SL, Collin OL, Jackson GP. Metastable atom-activated dissociation mass spectrometry: Leucine/isoleucine differentiation and ring cleavage of proline residues. *J Mass Spectrom*. 2009;44(8):1211-1223. doi:10.1002/jms.1598
38. Zhang L, Reilly JP. Peptide photodissociation with 157 nm light in a commercial tandem time-of-flight mass spectrometer. *Anal Chem*. 2009;81(18):7829-7838. doi:10.1021/ac9012557
39. Hoffmann WD, Jackson GP. Charge transfer dissociation (CTD) mass spectrometry of peptide cations using kiloelectronvolt helium cations. *J Am Soc Mass Spectrom*. 2014;25(11):1939-1943. doi:10.1007/s13361-014-0989-6
40. Li P, Jackson GP. Charge transfer dissociation (CTD) mass spectrometry of peptide cations: Study of charge state effects and side-chain losses. *J Am Soc Mass Spectrom*. 2017;28(7):1271-1281. doi:10.1007/s13361-016-1574-y
41. Ropartz D, Li P, Fanuel M, Giuliani A, Rogniaux H, Jackson GP. Charge transfer dissociation of complex oligosaccharides: Comparison with collision-induced dissociation and extreme ultraviolet dissociative photoionization. *J Am Soc Mass Spectrom*. 2016;27(10):1614-1619. doi:10.1007/s13361-016-1453-6
42. Chingin K, Makarov A, Denisov E, Rebrov O, Zubarev RA. Fragmentation of positively-charged biological ions activated with a beam of high-energy cations. *Anal Chem*. 2014;86(1):372-379. doi:10.1021/ac403193k
43. Bari S, Hoekstra R, Schlathölter T. Peptide fragmentation by keV ion-induced dissociation. *Phys Chem Chem Phys*. 2010;12(14):3376-3383. doi:10.1039/c004156b
44. Bari S, Hoekstra R, Schlathölter T. Fast side-chain losses in keV ion-induced dissociation of protonated peptides. *Int J Mass Spectrom*. 2011;299(1):64-70. doi:10.1016/j.ijms.2010.09.019
45. Hood C, Fuentes G, Patel H, Page K, Menakuru M, Park JH. Fast conventional Fmoc solid-phase peptide synthesis with HCTU. *J Pept Sci*. 2008;14(1):97-101. doi:10.1002/PSC.921
46. Niedermeyer THJ, Strohalm M. MMass as a software tool for the annotation of cyclic peptide tandem mass spectra. *PLoS ONE*. 2012;7(9):e44913 doi:10.1371/journal.pone.0044913
47. Strohalm M, Kavan D, Novák P, Volný M, Havlíček V. MMass 3: A cross-platform software environment for precise analysis of mass spectrometric data. *Anal Chem*. 2010;82(11):4648-4651. doi:10.1021/ac100818g
48. Strohalm M, Hassman M, Košata B, Kodíček M. MMass data miner: An open source alternative for mass spectrometric data analysis. *Rapid Commun Mass Spectrom*. 2008;22(6):905-908. doi:10.1002/rcm.3444
49. Robinson MR, Taliaferro JM, Dalby KN, Brodbelt JS. 193 nm ultraviolet photodissociation mass spectrometry for phosphopeptide characterization in the positive and negative ion modes. *J Proteome Res*. 2016;15(8):2739-2748. doi:10.1021/acs.jproteome.6b00289
50. Syka JE, Coon JJ, Schroeder MJ, Shabanowitz J, Hunt DF. Peptide and protein sequence analysis by electron transfer dissociation mass spectrometry. *Proc Natl Acad Sci USA*. 2004;101(26):9528-9533.
51. Zubarev RA, Kelleher NL, McLafferty FW. Electron capture dissociation of multiply-charged protein cations. A nonergodic process. *J Am Chem Soc*. 1998;120(16):3265-3266. doi:10.1021/ja973478k
52. Yu X, Zhong W. Differentiation of norvaline and valine in peptides by hot electron capture dissociation. *Anal Chem*. 2016;88(11):5914-5919. doi:10.1021/acs.analchem.6b00823
53. Zhang L, Cui W, Thompson MS, Reilly JP. Structures of α-type ions formed in the 157 nm photodissociation of singly-charged peptide ions. *J Am Soc Mass Spectrom*. 2006;17(9):1315-1321. doi:10.1016/j.jasms.2006.06.007
54. Cui W, Thompson MS, Reilly JP. Pathways of peptide ion fragmentation induced by vacuum ultraviolet light. *J Am Soc Mass Spectrom*. 2005;16(8):1384-1398. doi:10.1016/j.jasms.2005.03.050

SUPPORTING INFORMATION

Additional supporting information may be found in the online version of the article at the publisher's website.

How to cite this article: Edwards HM, Wu H-T, Julian RR, Jackson GP. Differentiation of leucine and isoleucine residues in peptides using charge transfer dissociation mass spectrometry (CTD-MS). *Rapid Commun Mass Spectrom*. 2022;36(5):e9246. doi:10.1002/rcm.9246